Development 138, 3907-3914 (2011) doi:10.1242/dev.070987

Hippo pathway regulation by cell morphology and stress fibers

Ken-Ichi Wada[1,2], Kazuyoshi Itoga[3], Teruo Okano[3], Shigenobu Yonemura[4] and Hiroshi Sasaki[1,2,*]

SUMMARY

The Hippo signaling pathway plays an important role in regulation of cell proliferation. Cell density regulates the Hippo pathway in cultured cells; however, the mechanism by which cells detect density remains unclear. In this study, we demonstrated that changes in cell morphology are a key factor. Morphological manipulation of single cells without cell-cell contact resulted in flat spread or round compact cells with nuclear or cytoplasmic Yap, respectively. Stress fibers increased in response to expanded cell areas, and F-actin regulated Yap downstream of cell morphology. Cell morphology- and F-actin-regulated phosphorylation of Yap, and the effects of F-actin were suppressed by modulation of Lats. Our results suggest that cell morphology is an important factor in the regulation of the Hippo pathway, which is mediated by stress fibers consisting of F-actin acting upstream of, or on Lats, and that cells can detect density through their resulting morphology. This cell morphology (stress-fiber)-mediated mechanism probably cooperates with a cell-cell contact (adhesion)-mediated mechanism involving the Hippo pathway to achieve density-dependent control of cell proliferation.

KEY WORDS: Hippo signaling, Cell morphology, F-actin, Mouse

INTRODUCTION

The Hippo signaling pathway is an evolutionarily conserved tumor-suppressor signaling pathway that plays an important role in regulation of cell proliferation (see Halder and Johnson, 2011; Pan, 2007; Reddy and Irvine, 2008; Saucedo and Edgar, 2007). Core Hippo pathway components are: protein kinases Mst1/2 (Hippo; *Drosophila* counterparts are shown in parentheses) and Lats1/2 (Warts), co-activator proteins Yap/Taz (Yorkie) and transcription factors Tead1-4 (Scalloped). In cultured cells, Hippo signals are involved in cell-density-dependent regulation of cell proliferation, which is also known as 'cell contact inhibition of proliferation' (Ota and Sasaki, 2008; Zhao et al., 2007). At low cell densities, weak Hippo signals allow nuclear Yap accumulation, which promotes cell proliferation by Tead activation. High cell densities induce strong Hippo signaling that suppresses cell proliferation by inhibiting nuclear Yap accumulation. Therefore, cell density regulates Hippo signaling, but the mechanisms by which cells detect density remain unknown.

Cell density changes alter cell-cell contact (adhesion) and cell morphology. At low cell densities, cell-cell contact frequencies or ratios of contacting to non-contacting membranes are low, and they are increased at high cell densities. Simultaneously, cells also change morphology in response to cell density. At low cell densities, cells are flat and spread, whereas at high densities they are round and compact. Therefore, both cell-cell contact (and adhesion) and cell morphology are candidate factors involved in the regulation of the Hippo signaling pathway.

[1]Department of Cell Fate Control, Institute of Molecular Embryology and Genetics, Kumamoto University, 2-2-1 Honjo, Kumamoto 860-0811, Japan. [2]Laboratory of Embryonic Induction, RIKEN Center for Developmental Biology, 2-2-3 Minatojima-minamimachi, Chuo-ku, Kobe, Hyogo 560-0047, Japan. [3]Institute of Advanced Biomedical Engineering and Science, Tokyo Women's Medical University, 8-1 Kawada-cho, Shinjuku, Tokyo 162-8666, Japan. [4]Electron Microscopy Laboratory, RIKEN Center for Developmental Biology, 2-2-3 Minatojima-minamimachi, Chuo-ku, Kobe, Hyogo 560-0047, Japan.

*Author for correspondence (sasaki@kumamoto-u.ac.jp)

Accepted 18 July 2011

Studies in *Drosophila* and mammals identified cell-cell adhesion molecules such as Fat (Bennett and Harvey, 2006; Cho et al., 2006; Silva et al., 2006; Tyler and Baker, 2007; Willecke et al., 2006), and junction-related proteins, such as merlin/NF2 (Hamaratoglu et al., 2006; Striedinger et al., 2008), Expanded (Hamaratoglu et al., 2006), Crumbs (Chen et al., 2010; Grzeschik et al., 2010; Ling et al., 2010; Robinson et al., 2010; Varelas et al., 2010), Angiomotin (Chan et al., 2011; Wang et al., 2010; Zhao et al., 2011) and α-catenin (Schlegelmilch et al., 2011; Silvis et al., 2011) as regulators of the Hippo pathway. However, little is known regarding the role of cell morphology in the regulation of the Hippo signaling pathway. A previous study showed that morphological manipulation of a single endothelial cell could alter cell proliferation (Chen et al., 1997). Considering that Hippo signals regulate cell proliferation, this finding is consistent with our hypothesis that cell morphology regulates the Hippo signaling pathway.

In this study, we investigated the role of cell morphology in regulation of Hippo signaling, and examined the effects independently from cell-cell contact or adhesion by manipulation of single-cell morphology. Our results demonstrate the importance of cell morphology in the regulation of Hippo signaling.

MATERIALS AND METHODS

Microdomain cell culture

Microdomains were fabricated as described elsewhere (Itoga et al., 2006) with modifications (Fig. 1D). Briefly, micro-patterned visible light was irradiated on to a photoresist-coated substrate to create a master mold for polydimethylsiloxane (PDMS) stamp preparation. PDMS stamps were placed on cell culture dishes and incubated with 0.6% agarose in 40% ethanol for 3 hours at room temperature to dry. After PDMS stamp removal, the culture dish was washed with 100% ethanol followed by rinses with sterile deionized water. The procedure created microscopic areas of various sizes for cell adhesion surrounded by a non-adhesive thin (~5 μm) agarose layer.

Before seeding onto microdomains, NIH3T3 cells were treated with 2 μg/ml mitomycin C for 3 hours to inhibit cell division and enhance cellular extension. After 18 hours, cells were fixed with 4% paraformaldehyde in phosphate-buffered saline (PFA-PBS) for further analyses.

Cell lines
NIH3T3 and MTD-1A (Hirano et al., 1987) cell lines were cultured in Dulbecco's modified Eagle's medium containing 4.5 g/l glucose supplemented with 10% fetal bovine serum. Enhanced green fluorescent protein (EGFP)-expressing NIH3T3 cells were generated by infection with the retroviral vector pMYs-IRES-EGFP (Kitamura et al., 2003).

Cell suspension
Low-density NIH3T3 cells were harvested by treatment with 0.05% trypsin at 37°C for 3 minutes. Cells were fixed with 4% PFA-PBS immediately after trypsinization or after incubation in culture medium for 10 minutes. Fixed cells were placed on poly-L-lysine (Sigma)-coated glass slides and processed for immunofluorescent staining.

Immunofluorescent staining
Immunofluorescent staining was performed with standard procedures using the following primary antibodies: rabbit anti-YAP1 (Ota and Sasaki, 2008), mouse anti-YAP (Abnova), rabbit anti-p-YAP (Cell Signaling), and mouse anti-HA (Santa Cruz). For phosphorylated YAP (p-YAP) staining, a phosphatase inhibitor cocktail (Nacalai Tesque, Kyoto, Japan) was added to the primary antibody solution at a 1:100 dilution. Microtubules, F-actin and nuclei were visualized with an FITC-conjugated anti-tubulin antibody (Sigma), Alexa-Fluor-488-phalloidin (Molecular Probes) and Hoechst 33258 (Dojindo), respectively.

Luciferase assay
One day before transfection, 5×10^4 NIH3T3 cells were seeded in a 35 mm dish and then a transfection mixture containing 1.44 μg 8× GTIIC-Luc or pδ51-Luc, 0.16 μg pCAG-β-gal and 4 μl Lipofectamine 2000 was added. After 3 hours incubation, cells were treated with 2 μg/ml mitomycin C for 3 hours, followed by treatment with 1 μM cytochalasin D (CytoD) or 0.05% dimethyl sulfoxide (DMSO) for 12 hours. Cell lysate preparation, measurements of luciferase and β-galactosidase activities were performed as described elsewhere (Sasaki et al., 1997).

Plasmids
The plasmids pcDNA-HA-Lats2, pCMV-EGFP, 8×GTIIC-Luc and pδ51-Luc are described elsewhere (Ota and Sasaki, 2008). A mutation in Lats2 (Asp767Ala) was introduced into pcDNA-HA-Lats2 to construct pcDNA-HA-Lats2-KD. The plasmids pCAG-HA-Yap and pCAG-HA-YapSer112Ala (YapS112A) were constructed by inserting a GS linker (three repeats of GGGGS) sequence between the HA tag and Yap (or YapS112A). The β-galactosidase gene was subcloned from pCS2-β-gal (Ota and Sasaki, 2008) into the pCAG vector to construct pCAG-β-gal.

Transient expression of Hippo components
For manipulation of Lats activity, NIH3T3 cells were seeded into 24-well plates (4×10^4 cells/well) the day before transfection. Transfection mixtures containing 0.4 μg pcDNA-HA-Lats2, pcDNA-HA-Lats2-KD or pCMV-EGFP and 1 μl Lipofectamine 2000 were added to cells. After 3 hours incubation, $0.5\text{-}1.0\times10^5$ transfected cells were re-plated on to a 35 mm dish and cultured for 18 hours. For Yap transfection, 2×10^5 cells were seeded in a 35 mm dish a day before transfection with 20 ng pCAG-HA-Yap or pCAG-HA-YapS112A, 480 ng of pBluescript and 1.3 μl Lipofectamine 2000. After 3 hours incubation, $0.5\text{-}1.0\times10^5$ transfected cells were re-plated onto a 35 mm dish and cultured for 1 day.

Phos-tag-polyacrylamide gel electrophoresis (phos-tag-PAGE) and western blot analyses
After a wash in PBS, cells were lysed with 2.5% sodium dodecyl sulfate (SDS) sample buffer [2.5% SDS, 10% glycerol, 62.5 mM Tris-HCl pH 6.8, 5% 2-mercaptoethanol, 1 mM dithiothreitol, 50 mM NaF, 0.2 mM sodium vanadate and Complete EDTA-free protease inhibitor (Roche)]. For preparation of dephosphorylated samples, cells were fixed with 10% trichloroacetic acid for 15 minutes at 4°C, washed three times with Tris-buffered saline (pH 7.5) and then incubated with 4 IU/μl lambda protein phosphatase (New England Biolab) for 2 hours at 30°C before lysis. SDS-polyacrylamide gels (10%) containing 20 μM phos-tag (NARD Institute, Japan) were prepared according to the manufacturer's instructions and used for electrophoresis. Western blotting was performed using a standard protocol.

Image data quantification
Cell area, stress fiber length and average p-Yap signal intensities within the entire region of the cells were measured with AxioVision Rel. 4.6 software (Zeiss). Background signals were subtracted from p-Yap signal measurements.

Statistics
Statistical data were analyzed by an unpaired two-tailed *t*-test or one-way ANOVA followed by Tukey's multiple comparison test, as appropriate, using Prism5 statistical software (GraphPad). A value of $P<0.05$ was regarded as significant.

RESULTS AND DISCUSSION

Cell morphology regulates subcellular Yap localization
Considering that Yap is regulated by cell morphology, correlations may exist between cell density, morphology and Yap distribution. Therefore, we examined the correlation between the area covered by each cell (hereafter designated as 'cell area') and Yap distribution in mouse embryonic fibroblast NIH3T3 cells at various cell densities. We used the NIH3T3 cell line because of distinct contact inhibition and Yap regulation (Ota and Sasaki, 2008). Under experimental conditions, cells reached confluency at day 3 and ceased proliferation (see Fig. S1 in the supplementary material). Cell area was measured using the areas of EGFP-expressing cells sparsely mixed in the cultures, which significantly decreased at day 3 (Fig. 1B). This indicated that an increase in cell density reduced cell area. Consistent with previous studies, Yap was mostly localized in nuclei at low cell densities and in the cytoplasm at confluence (Fig. 1A). Yap distribution patterns were classified as nuclear (nucleus>cytoplasm), diffuse (nucleus and cytoplasm) and cytoplasmic (nucleus<cytoplasm). Nuclear-Yap-expressing cell areas were significantly larger compared with those of the cells expressing cytoplasmic Yap (Fig. 1C). Therefore, there is a correlation between cell density, cell area (morphology) and Yap distribution.

However, under normal cell culture conditions, changes in cell density simultaneously alter cell area and cell-cell contact. To clarify the role of cell area independent of cell-cell contact, we fabricated micropatterned cell adhesive areas called microdomains (Fig. 1D) and cultured a single NIH3T3 cell on each microdomain. Using variously sized microdomains, we manipulated the area (morphology) of a single cell without cell-cell contact (Fig. 1D). On small domains (e.g. 20×20 μm), cells were compact and round, whereas on larger domains (e.g. 70×70 μm) cells were spread and flat (Fig. 1D,E). On small domains, Yap was mostly cytoplasmic, whereas Yap was nuclear on large domains (Fig. 1E,F). Yap distribution patterns gradually changed with domain sizes. However, there appeared to be a threshold using domains between 30×30 μm and 40×40 μm. Cells on domains larger than the threshold did not show cytoplasmic Yap, whereas cells on domains that were smaller did not show nuclear Yap (Fig. 1F). These results suggest that cell area (morphology) regulates Yap distribution independent of cell-cell contact or adhesion.

The effect of cell morphology on Yap distribution was also observed by detaching cells from culture dishes. Cells cultured at a low cell density with nuclear Yap were detached from dishes and cultured in suspension for 10 minutes. Cells then became rounded

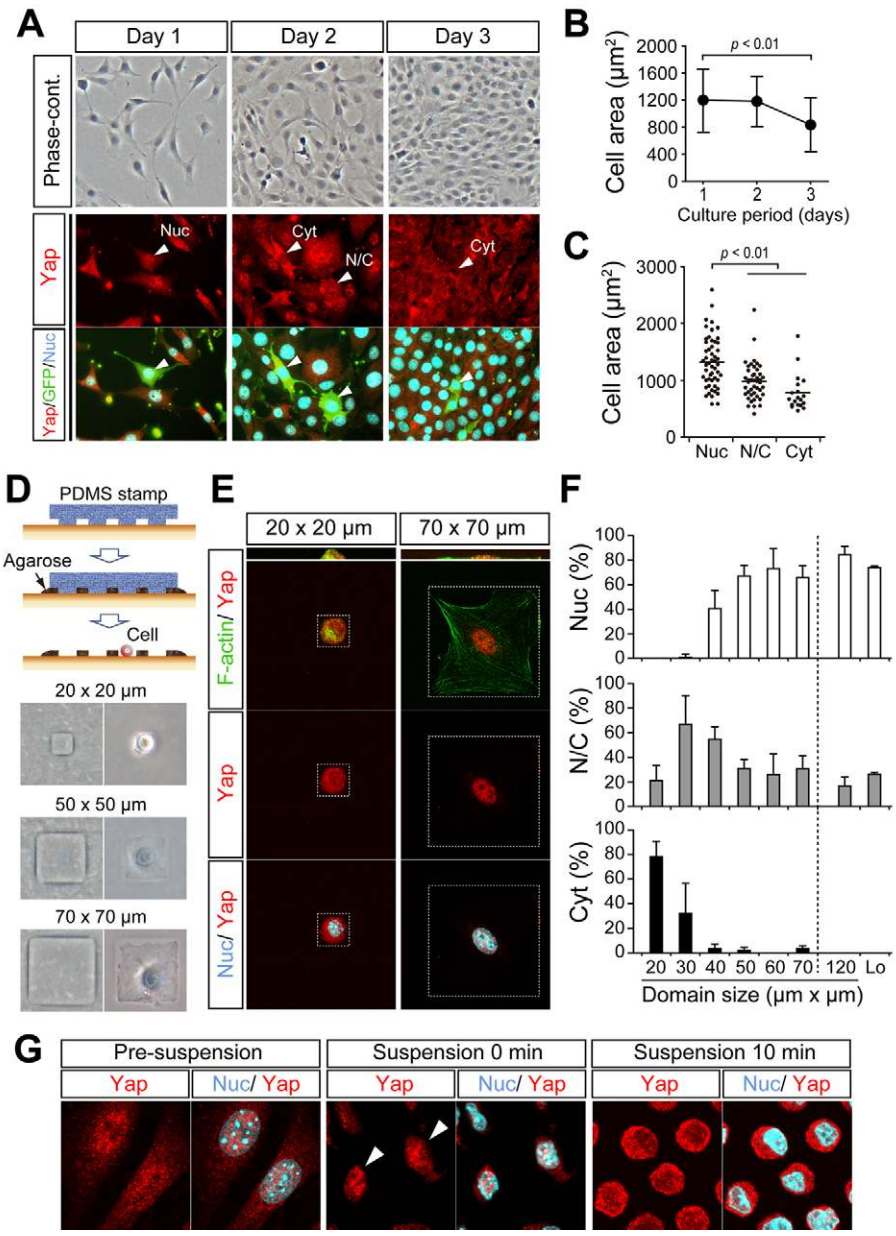

Fig. 1. Cell morphology regulates Yap. (**A-C**) Relationship between cell area and subcellular Yap distribution in normal cell cultures. (A) Phase-contrast and fluorescent images of NIH3T3 cells. Yap distribution patterns were classified as mainly nuclear (Nuc), diffuse (nucleus and cytoplasm; N/C) and mainly cytoplasmic (Cyt). Representative cells showing each pattern are indicated by arrowheads with abbreviations. (B) Changes in cell area during cell culture. Values are means ± standard deviations (s.d.). (C) Relationship between the Yap distribution pattern and cell area. (**D-F**) Relationship between cell area and subcellular Yap distribution in microdomain cell culture. (D) Microdomain cell culture system. Upper panels: schematic illustration of microdomain production. Lower panels: examples of fabricated microdomains (left) and the morphology of cells cultured on microdomains (right). (E) Confocal images of cells on microdomains. F-actin (green) was used to visualize cell morphology. Dotted lines indicate the microdomain area. The top panels are confocal *z*-sectional views. Other panels are single *xy*-sections. (F) Relationship between domain size and Yap distribution pattern. Cells did not cover the 120×120 μm domain area. Lo is normal low-density culture. Data were collected from three independent experiments, analyzing ≥20 cells for each domain size. Values are means ± s.d. (**G**) Dynamics of Yap regulation by cell morphology. Yap is still present in the nuclei of suspended cells immediately after detachment (center, arrowheads). In A,E and G Nuc in blue indicates the staining of the nuclei not the location of Yap.

and the Yap was cytoplasmic (Fig. 1G). The lack of cell-cell contacts, further supports the hypothesis that cell morphology regulates Yap localization and the regulatory pathway is rapidly initiated.

Stress fibers regulate Yap downstream of cell morphology

Cytoskeleton proteins, including F-actin, determine cell morphology. To determine the molecular mechanisms by which cell morphology regulates Yap localization, we examined F-actin distribution in normal cell cultures (Fig. 2A). At low cell densities, the F-actin in stress fibers is thick and abundant. However, at high cell densities, stress fibers were thin and less evident. In addition, essentially no stress fibers were observed in cells detached from culture dishes (Fig. 2A). Interestingly, the quantity of F-actin in the cell periphery was relatively unchanged. Therefore, there appears to be a correlation between cell density (and therefore morphology) and stress fiber quantity.

To investigate this possible correlation, we analyzed stress fiber quantity using microdomains. On 20×20 μm domains, F-actin staining appeared punctate and stress fibers were barely observed. However, on 50×50 μm domains, stress fibers were clearly present (Fig. 2B). Stress fiber lengths per unit area increased as larger microdomains were used (Fig. 2B). Similar to normal cell culture, F-actin signal in the cell periphery was not significantly altered. Therefore, stress fiber quantity changes in response to changes in morphology.

To evaluate the role of stress fibers in Yap localization, we disrupted F-actin by treatment with anti-actin drugs (Fig. 2C,D and see Fig. S2 in the supplementary material). Treatment of cells with CytoD or latrunculin A (LatA) for 1 hour resulted in reduced stress fibers and nuclear Yap (Fig. 2C,D and see Fig. S2 in the supplementary material). Similarly, treatment of cells with the myosin inhibitors, blebbistatin (Blebb), ML-7 and Y27632, which inhibit, myosin II ATPase, a myosin light-chain kinase, and Rho kinase, respectively, also reduced stress fibers and nuclear Yap

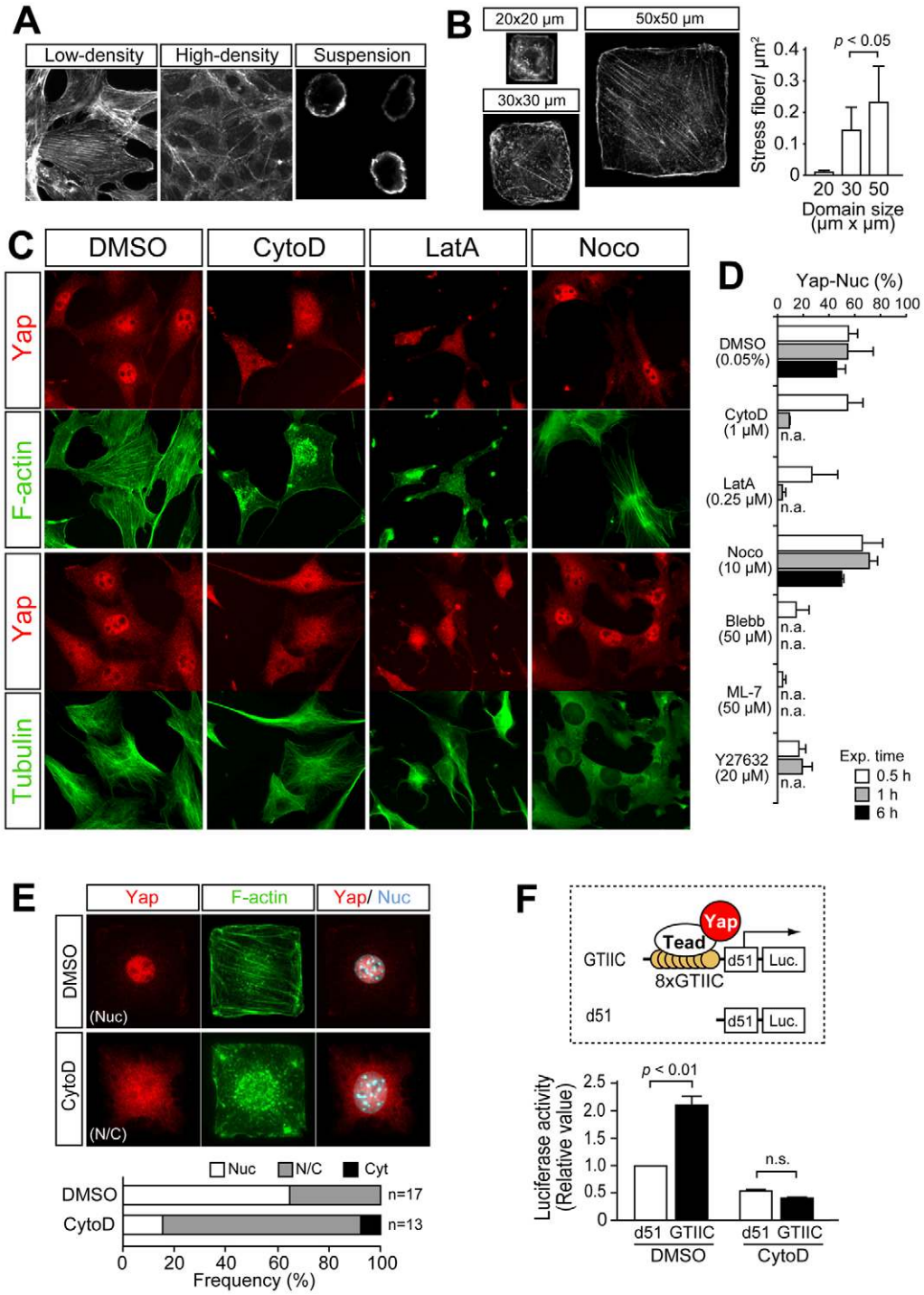

Fig. 2. Stress fiber promotes nuclear Yap downstream of cell morphology. (**A**) F-actin distribution in NIH3T3 cells. The panel labeled Suspension (right) shows cells detached from culture dishes for 10 minutes. (**B**) F-actin distribution in NIH3T3 cells cultured on different sized microdomains. Stress fibers increase in proportion to the cell area increase. Note that the punctate signals and the signals at the cell edges are not from stress fibers. The graph shows the relationship between domain sizes and stress fiber lengths per unit area. Values are means ± s.d. (**C-E**) F-actin is required for nuclear Yap accumulation. (C) Images showing the effect of actin and microtubule inhibiting drugs on the cytoskeleton and nuclear Yap localization. CytoD, cytocalasin D; LatA, latrunculin A; Noco, nocodazole. Merged images of Yap and nuclear staining are shown in Fig. S2 in the supplementary material. (D) Graph summarizing the effects of various drugs on nuclear Yap localization. Percentage of cells with nuclear Yap (Yap-Nuc) are shown. Blebb, blebbistatin. The concentrations of the reagents are indicated in parentheses. The duration of reagent treatment is indicated by the color of the bars (see key). Values are means ± s.d. from three independent experiments with ≥20 cells in each experiment. n.a., not analyzed. (E) Effects of CytoD on NIH3T3 cells cultured on 50×50 μm domains. Yap distribution was altered by treatment with CytoD without changing the cell area. The graph summarizes the distribution of Yap patterns in control (DMSO) and CytoD-treated cells. The abbreviations for Yap distribution patterns are as in Fig. 1. (**F**) Reduction of transcriptional activity of endogenous Tead proteins by CytoD treatment. Schematic presentation of the Tead-reporter and the control plasmids used in this study is shown in the upper panel. GTIIC is a Tead-binding motif. Results of the luciferase assay are shown in the lower panel. Values are means ± s.d. from two independent experiments.

(Fig. 2D and see Fig. S3 in the supplementary material). These results suggest that stress fibers consisting of F-actin are required for nuclear Yap localization. Importantly, cells with disrupted F-actin had normal microtubules, suggesting that the required cytoskeleton protein is specifically F-actin (Fig. 2C). Indeed, microtubule disruption with nocodazole (Noco) did not alter stress fibers, and nuclear Yap was clearly observed (Fig. 2C,D and see Fig. S2 in the supplementary material).

To elucidate the relationship between cell morphology and stress fibers in Yap localization, we performed drug treatments using cells that were cultured on microdomains. The majority of cells showed clear nuclear Yap on 50×50 μm domains. CytoD treatment disrupted stress fibers, while cells maintained their original area and lost nuclear Yap localization (Fig. 2E). This result suggests that stress fibers function downstream of cell morphology.

Because Yap regulates cell proliferation by modulation of Tead expression, we examined endogenous Tead activity using a reporter containing Tead binding sites (8×GT-IIC-Luc) (Ota and Sasaki, 2008). Consistent with reduced nuclear Yap, Tead activity was also reduced by CytoD treatment (Fig. 2F). These results suggest that F-actin promotes nuclear Yap accumulation downstream of cell morphology and that stress fibers consisting of F-actin are the prime candidate for correlating morphology to Yap regulation.

Stress fibers regulate Yap through the Hippo pathway upstream of, or at, Lats

To examine whether stress fibers function through the Hippo pathway, we manipulated the activity of Lats protein kinase by overexpression of Lats2 or a kinase-defective form of Lats2 (Lats2-KD) that is dominant negative for Lats1/2 (Nishioka et al., 2009). Lats phosphorylates five serine residues including S112 in mouse Yap and inhibits nuclear localization (Zhao et al., 2007). We found that Lats2-KD reduced phosphorylation of YapS112 (p-Yap; Fig. 3A,C) and Lats2 reduced nuclear Yap (Fig. 3A,B).

To examine the relationship between stress fibers and Hippo signaling, we treated the transfected cells with CytoD. In control EGFP-transfected cells, stress fiber disruption by CytoD treatment reduced nuclear Yap (Fig. 3A,B). Lats2 also reduced nuclear Yap and was not significantly affected by CytoD (Fig. 3A,B). Conversely, in Lats2-KD-expressing cells, nuclear Yap was maintained following CytoD treatment (Fig. 3A,B). Therefore, Lats is epistatic to stress fibers. The most probable explanation of these results is that stress fibers regulate Yap through Hippo signaling, which acts upstream or on Lats, although the possibility that actin acts in parallel to Lats cannot be excluded.

To further investigate the hypothesis that Lats is epistatic to F-actin, we studied the role of S112 phosphorylation by analyzing the distribution of a phosphorylation-defective form of Yap (YapS112A). At low cell densities, exogenously expressed HA-tagged Yap showed a similar distribution to endogenous Yap. HA-Yap was mostly localized in nuclei and CytoD treatment suppressed nuclear localization (Fig. 3D,E). By contrast, HA-YapS112A showed strong nuclear localization in all transfected cells and the pattern was not affected by CytoD (Fig. 3D,E). Therefore, YapS112 phosphorylation by Lats is required for stress fiber-dependent Yap localization.

Phosphorylation of S112 is not sufficient to exclude Yap from nuclei

Phosphorylation of S112 is important for suppression of nuclear Yap because p-S112 binds to the scaffolding protein 14-3-3, which promotes cytoplasmic retention of bound proteins (Zhao et al.,

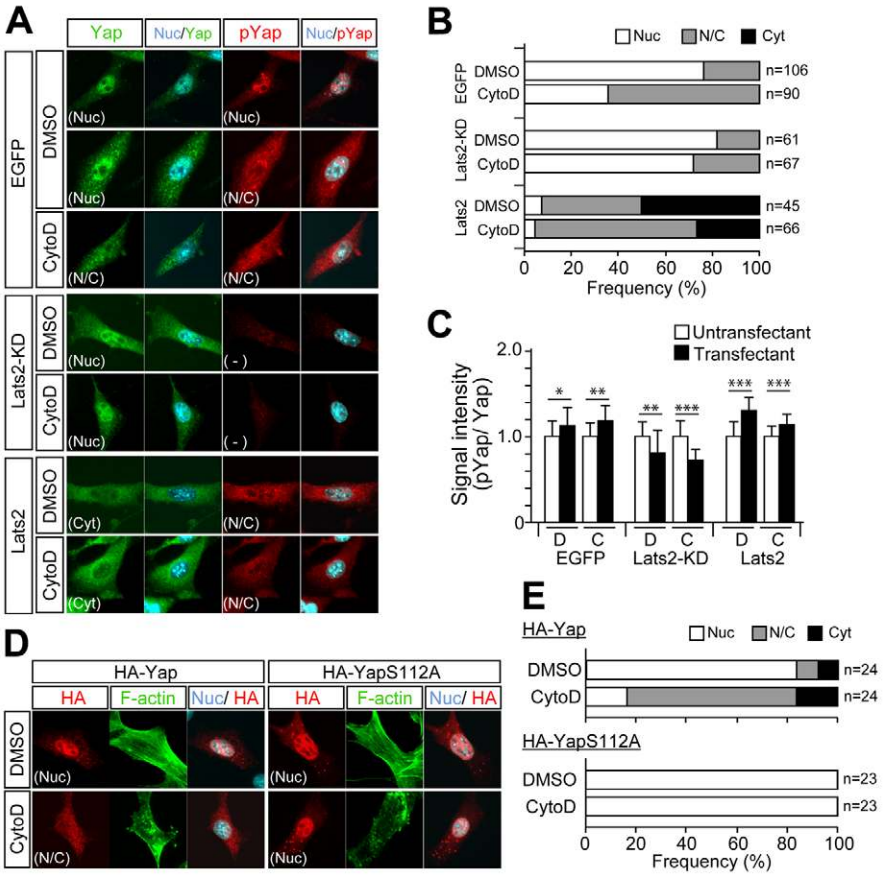

Fig. 3. F-actin regulates Yap through the Hippo pathway. (**A-C**) Lats is epistatic to F-actin. (A) Representative cells showing the effects of dominant-negative Lats2 (Lats2-KD) and Lats2 on Yap in CytoD-treated cells. p-Yap is Yap phosphorylated at S112. The abbreviations for Yap distribution patterns are as in Fig. 1. and are shown in the corner of the panels. (B) Graph summarizing the effects on Yap distribution. The Yap distribution pattern was classified and abbreviated as shown in Fig. 1A. (C) Graph showing the relative changes in p-Yap signal levels expressed as the ratio of the p-Yap signal to total Yap signal. The average value of non-transfected cells was set at 1.0. Values are means ± s.d. from >18 cells for each cell type. *P<0.05; **P<0.01; ***P<0.001. (**D**,**E**) Requirement for pS112 in actin-dependent Yap regulation. (D) Representative cells showing the effects of F-actin disruption on Yap-S112A regulation. The Yap distribution pattern is given in the corner of the panels. (E) Graph summarizing the distribution of exogenously expressed Yap and Yap-S112A in CytoD-treated cells.

2007). We also observed that phosphorylation of this site is required for Yap exclusion from the nucleus (Fig. 3D,E). Unexpectedly, we also observed a small number of normal cells that express phosphorylated YapS112 (p-Yap) in the nucleus (Fig. 3A, top). Therefore, we further studied the role of phosphorylation of S112 in Yap localization.

We found that at low cell densities, Yap was localized to the nucleus and its level in the cytoplasm was low. In these cells, p-Yap also had a strong signal in the nucleus but the nuclear/cytoplasmic ratio was lower than that of Yap (Fig. 4A,B, left), indicating that not all the nuclear Yap protein is phosphorylated at S112. Clear nuclear p-Yap was also observed in an epithelial cell line, MTD-1A (Fig. 4A). At high cell densities, Yap was localized to the cytoplasm and its level in the nucleus was low. In these cells, p-Yap was also mostly observed in the cytoplasm (Fig. 4A,B, left). CytoD treatment of low-density cells resulted in both Yap and p-Yap becoming diffusible (Fig. 4A,B, right). Therefore, the distribution pattern of p-Yap is similar to that of Yap, although the nuclear/cytoplasmic ratio of p-Yap tended to be lower than that of Yap. The specificity of an anti-p-Yap antibody was confirmed by western blotting and immunohistochemistry. Using western blotting, the anti-p-Yap antibody produced a single band corresponding to the size of Yap (see Fig. S4 in the supplementary material), which was not present in lysates pre-treated with lambda protein phosphatase (Fig. 4C). Similarly, the anti-p-Yap antibody did not produce immunohistochemical signals from cells pre-treated with protein phosphatase after fixation (Fig. 4A). These results suggest that S112-phosphorylated Yap proteins are present in the nuclei of normal low-density cells.

Cell morphology and F-actin regulate the phosphorylation level of Yap

Our results suggest that phosphorylation of S112 is not sufficient, but is still required, for Yap exclusion from the nucleus. Because Yap possesses many phosphorylation sites for Lats (Dong et al., 2007; Zhao et al., 2007), we hypothesized that Yap phosphorylation at sites other than S112 is important for Yap exclusion from the nucleus. If this hypothesis was correct, a correlation would exist between subcellular Yap localization and Yap phosphorylation levels. Yap phosphorylation levels were analyzed with phos-tag-

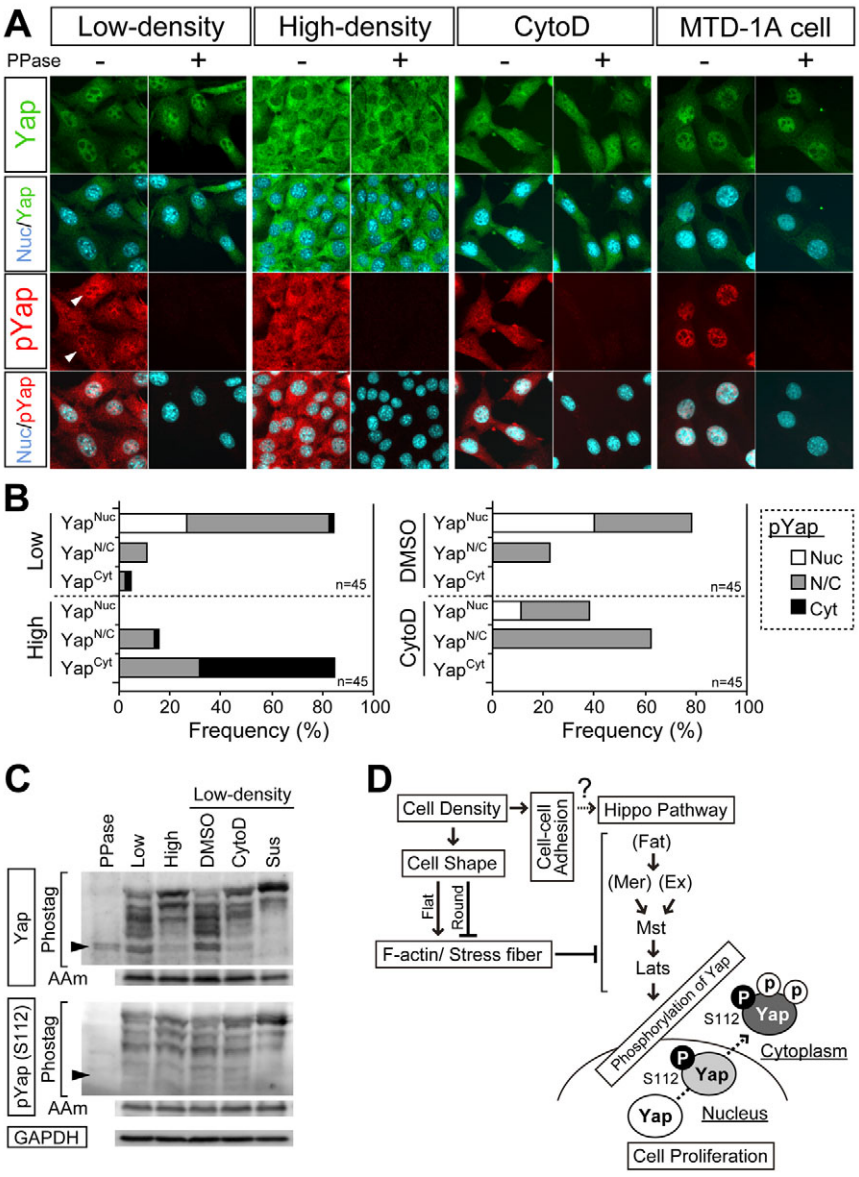

Fig. 4. Phosphorylation at positions other than S112 in Yap is required for Yap exclusion from the nucleus. (**A**,**B**) p-Yap (phosphorylated at S112) is localized in the nucleus. (A) Distribution patterns of Yap and p-Yap in NIH3T3 cells and low-density MTD-1A cells under various conditions. Signals for p-Yap were not detected in cells pre-treated with lambda protein phosphatase (PPase +) before antibody reaction, demonstrating the specificity of the antibody. Arrowheads indicate nuclear p-Yap localization. (B) Graphs summarizing distribution patterns of Yap and p-Yap at low and high cell densities (left) and in CytoD-treated cells (right). To simultaneously show the distribution of Yap and p-Yap in a single graph, the following criteria were applied. Cells were first classified according to the Yap distribution pattern as described in Fig. 1A, and the percentage of each class was shown in a bar graph. Cells showing each class of Yap distribution pattern (i.e. each bar) were further classified according to the p-Yap distribution pattern. Based on the p-Yap classification, each bar, representing each Yap class, was subdivided according to the p-Yap class shown in the right panel (see key). (**C**) Cell morphology and F-actin regulate the phosphorylation level of Yap. Phos-tag-PAGE showing the phosphorylation level of Yap. PPase, samples pre-treated with lambda protein phosphatase; Low, low-density cells; High, high-density cells; DMSO, low-density cells treated with 0.05% DMSO for 1 hour; CytoD, low-density cells treated with 1 μM CytoD for 1 hour; Sus, low-density cells in suspension culture for 10 minutes. Conventional SDS-PAGE is also shown (AAm). Arrowheads indicate the position of non-phosphorylated Yap. (**D**) Model of density-dependent Yap regulation (see text for details).

PAGE, in which the mobilities of phosphorylated proteins are reduced relative to the degree of phosphorylation. We observed that at low cell densities, and consistent with nuclear p-Yap localization, the majority of the Yap protein was phosphorylated at various levels and the non-phosphorylated protein was insignificant (Fig. 4C, Low). At high cell densities, Yap protein was highly phosphorylated (Fig. 4C, High). Consistent with the reduction of nuclear Yap, stress fiber disruption by CytoD treatment or by cell detachment, resulting in a rounded cell morphology and increased phosphorylation of Yap (Fig. 4C, CytoD, Sus). Total p-Yap signal intensities observed by normal SDS-PAGE were not significantly different (Fig. 4C, AAm), which supports the hypothesis that p-S112 by itself does not regulate subcellular localization of Yap, and that additional phosphorylation promotes nuclear exclusion. These results, from dissociated cells, demonstrate that cell-cell adhesion is not involved in activation of the Hippo pathway. Therefore, cell density, stress fibers/F-actin and cell morphology regulate Yap phosphorylation, and there is a correlation between increased phosphorylation and a reduction in nuclear Yap.

Hippo pathway regulation by cell morphology and stress fibers

Based on these and other findings, we propose a model of the regulation of the Hippo pathway by cell morphology (Fig. 4D). In cell culture, cell proliferation is regulated by cell density, which is known as 'cell contact inhibition of proliferation', and it is regulated by Hippo signaling. Cell density alters morphology and cell-cell contact, and we demonstrated the importance of cell morphology in the regulation of Hippo signaling. At low cell densities, cells are flat and spread, and this morphology promotes the formation of stress fibers (F-actin). Stress fibers inhibit the Hippo pathway upstream of or at Lats, thereby reducing Yap phosphorylation and promoting nuclear Yap accumulation. In the nucleus, Yap binds to the Tead family of transcription factors and promotes cell proliferation. By contrast, at high cell densities, cells are compact and tall (or round), which reduces stress fibers and activates Hippo and Lats. Active Lats promotes phosphorylation of Yap. The presence of p-Yap is a prerequisite, but is not sufficient, to exclude Yap from nuclei; a higher level of phosphorylation does exclude Yap from nuclei.

Although in the current study we did not address the role of cell-cell contact and adhesion in Hippo signaling regulation, the involvement of merlin/NF2 in the regulation of Yap and contact inhibition of proliferation (Striedinger et al., 2008; Zhang et al., 2008; Zhao et al., 2007), and the association of merlin with the junction protein angiomotin (Amot) (Yi et al., 2011) suggest that cell-cell adhesion is important. It is probable that both cell morphology and cell-cell contact-mediated mechanisms operate in parallel and converge for Lats activation to regulate Yap. Alternatively, cell morphology and cell-cell contact information might converge to activate stress fiber (F-actin) formation that then regulates Hippo signaling. In support of this hypothesis, junction proteins, e.g. cadherins, are linked to actin fibers by adaptor proteins (for a review, see Meng and Takeichi, 2009). Recent studies of *Drosophila* also suggest Hippo pathway suppression by F-actin (Fernandez et al., 2011; Sansores-Garcia et al., 2011). F-actin probably functions as a scaffold for Hippo pathway components, and interactions with F-actin regulate signaling. Indeed, several Hippo pathway components, including Mst1/2 (Densham et al., 2009), merlin/NF2 (McCartney et al., 2000) and Amot (Ernkvist et al., 2006; Gagne et al., 2009), bind to actin, and Mst1/2 is activated upon F-actin depolymerization (Densham et al., 2009).

During the preparation of this paper, other group also reported that cell morphology and F-actin regulate Yap (Dupont et al., 2011). Interestingly, however, their results show that this mechanism is independent of the Hippo pathway, which is different from our results. We showed that Lats is epistatic to F-actin, and that one of the Lats phosphorylation sites of Yap, S112, is required for regulation of Yap by F-actin. Our results are also consistent with the results of a *Drosophila* study showing that the Lats homolog Warts is epistatic to F-actin (Sansores-Garcia et al., 2011). The reason for such differences between studies remains elusive.

Changes in cell morphology and stress fiber quantity are accompanied by changes in physical forces or the tension that cells receive and generate. Without external forces, cells are spherical. Cells become flat and spread because of external stretching forces or the forces generated at the cell periphery, with stress fibers being produced to counterbalance the external and/or internal forces. Therefore, physical forces and/or tensions that cells receive or generate might also regulate the Hippo pathway. In support of this hypothesis, myocardial cells in E8.5-10.5 mouse embryos actively beat and show stronger nuclear Yap signals as well as Tead1 accumulation compared with cells of other tissues (Ota and Sasaki, 2008). In addition, mutation of Tead1 is embryonic lethal because of severe defects in myocardium cell proliferation (Chen et al., 1994; Sawada et al., 2008). Considering the correlation between physical force and Hippo signaling, the Hippo signaling pathway may be involved in load-induced myofiber hypertrophy, whereby physical forces induce muscle protein synthesis. Indeed, Tead proteins bind to M-CAT sequence motifs and regulate numerous cardiac and skeletal muscle-specific genes such as cardiac troponin C, T and I as well as myosins (for a review, see Yoshida, 2008), suggesting their involvement in muscle plasticity.

In conclusion, we identified cell morphology as an important factor in the regulation of Hippo signaling. In embryonic and adult tissues, cells have a diverse morphology and there appears to be a correlation between cell morphology and Hippo signaling. In pregastrulation embryos, epiblast cells are columnar and the surrounding primitive endodermal cells are flat and thin. Hippo is active in epiblast cells and inactive in primitive endoderm (Varelas et al., 2010). In preimplantation embryos, Hippo signaling is inactive in the outer flat trophectodermal cells and active in the inner compact cells (Nishioka et al., 2009). The mechanism by which cell morphology regulates Hippo signaling in vivo, and the mechanisms of cell morphology and tension and/or force signal integration with cell-cell contact and adhesion are unknown and are areas of research to be addressed in the future.

Acknowledgements

We thank H. Mamada (Institute of Molecular Embryology and Genetics, Kumamoto University, Kumamoto, Japan) for the GFP-expressing cell line and T. Kitamura (The Institute of Medical Science, The University of Tokyo, Japan) for reagents. This work was supported by grants from RIKEN, Uehara Memorial Foundation, and by Grants-in-Aid for Scientific Research from MEXT (21116003) and JSPS (23247036) to H.S., and from JSPS to K.I.W. (23770236).

Competing interests statement

The authors declare no competing financial interests.

Supplementary material

Supplementary material for this article is available at
http://dev.biologists.org/lookup/suppl/doi:10.1242/dev.070987/-/DC1

References

Bennett, F. C. and Harvey, K. F. (2006). Fat cadherin modulates organ size in *Drosophila* via the Salvador/Warts/Hippo signaling pathway. *Curr. Biol.* **16**, 2101-2110.

Chan, S. W., Lim, C. J., Chong, Y. F., Venkatesan Pobbati, A., Huang, C. and Hong, W. (2011). Hippo pathway-independent restriction of TAZ and YAP by angiomotin. *J. Biol. Chem.* **286**, 7018-7026.
Chen, C. L., Gajewski, K. M., Hamaratoglu, F., Bossuyt, W., Sansores-Garcia, L., Tao, C. and Halder, G. (2010). The apical-basal cell polarity determinant Crumbs regulates Hippo signaling in *Drosophila*. *Proc. Natl. Acad. Sci. USA* **107**, 15810-15815.
Chen, C. S., Mrksich, M., Huang, S., Whitesides, G. M. and Ingber, D. E. (1997). Geometric control of cell life and death. *Science* **276**, 1425-1428.
Chen, Z., Friedrich, G. A. and Soriano, P. (1994). Transcriptional enhancer factor 1 disruption by a retroviral gene trap leads to heart defects and embryonic lethality in mice. *Genes Dev.* **8**, 2293-2301.
Cho, E., Feng, Y., Rauskolb, C., Maitra, S., Fehon, R. and Irvine, K. D. (2006). Delineation of a Fat tumor suppressor pathway. *Nat. Genet.* **38**, 1142-1150.
Densham, R. M., O'Neill, E., Munro, J., Konig, I., Anderson, K., Kolch, W. and Olson, M. F. (2009). MST kinases monitor actin cytoskeletal integrity and signal via c-Jun N-terminal kinase stress-activated kinase to regulate p21Waf1/Cip1 stability. *Mol. Cell. Biol.* **29**, 6380-6390.
Dong, J., Feldmann, G., Huang, J., Wu, S., Zhang, N., Comerford, S. A., Gayyed, M. F., Anders, R. A., Maitra, A. and Pan, D. (2007). Elucidation of a universal size-control mechanism in *Drosophila* and mammals. *Cell* **130**, 1120-1133.
Dupont, S., Morsut, L., Aragona, M., Enzo, E., Giulitti, S., Cordenonsi, M., Zanconato, F., Le Digabel, J., Forcato, M., Bicciato, S. et al. (2011). Role of YAP/TAZ in mechanotransduction. *Nature* **474**, 179-183.
Ernkvist, M., Aase, K., Ukomadu, C., Wohlschlegel, J., Blackman, R., Veitonmaki, N., Bratt, A., Dutta, A. and Holmgren, L. (2006). p130-angiomotin associates to actin and controls endothelial cell shape. *FEBS J.* **273**, 2000-2011.
Fernandez, B. G., Gaspar, P., Bras-Pereira, C., Jezowska, B., Rebelo, S. R. and Janody, F. (2011). Actin-capping protein and the Hippo pathway regulate F-actin and tissue growth in *Drosophila*. *Development* **138**, 2337-2346.
Gagne, V., Moreau, J., Plourde, M., Lapointe, M., Lord, M., Gagnon, E. and Fernandes, M. J. (2009). Human angiomotin-like 1 associates with an angiomotin protein complex through its coiled-coil domain and induces the remodeling of the actin cytoskeleton. *Cell Motil. Cytoskeleton* **66**, 754-768.
Grzeschik, N. A., Parsons, L. M., Allott, M. L., Harvey, K. F. and Richardson, H. E. (2010). Lgl, aPKC, and Crumbs regulate the Salvador/Warts/Hippo pathway through two distinct mechanisms. *Curr. Biol.* **20**, 573-581.
Halder, G. and Johnson, R. L. (2011). Hippo signaling: growth control and beyond. *Development* **138**, 9-22.
Hamaratoglu, F., Willecke, M., Kango-Singh, M., Nolo, R., Hyun, E., Tao, C., Jafar-Nejad, H. and Halder, G. (2006). The tumour-suppressor genes NF2/Merlin and Expanded act through Hippo signalling to regulate cell proliferation and apoptosis. *Nat. Cell Biol.* **8**, 27-36.
Hirano, S., Nose, A., Hatta, K., Kawakami, A. and Takeichi, M. (1987). Calcium-dependent cell-cell adhesion molecules (cadherins): subclass specificities and possible involvement of actin bundles. *J. Cell Biol.* **105**, 2501-2510.
Itoga, K., Kobayashi, J., Yamato, M., Kikuchi, A. and Okano, T. (2006). Maskless liquid-crystal-display projection photolithography for improved design flexibility of cellular micropatterns. *Biomaterials* **27**, 3005-3009.
Kitamura, T., Koshino, Y., Shibata, F., Oki, T., Nakajima, H., Nosaka, T. and Kumagai, H. (2003). Retrovirus-mediated gene transfer and expression cloning: powerful tools in functional genomics. *Exp. Hematol.* **31**, 1007-1014.
Ling, C., Zheng, Y., Yin, F., Yu, J., Huang, J., Hong, Y., Wu, S. and Pan, D. (2010). The apical transmembrane protein Crumbs functions as a tumor suppressor that regulates Hippo signaling by binding to Expanded. *Proc. Natl. Acad. Sci. USA* **107**, 10532-10537.
McCartney, B. M., Kulikauskas, R. M., LaJeunesse, D. R. and Fehon, R. G. (2000). The neurofibromatosis-2 homologue, Merlin, and the tumor suppressor expanded function together in *Drosophila* to regulate cell proliferation and differentiation. *Development* **127**, 1315-1324.
Meng, W. and Takeichi, M. (2009). Adherens junction: molecular architecture and regulation. *Cold Spring Harb. Perspect. Biol.* **1**, a002899.
Nishioka, N., Inoue, K., Adachi, K., Kiyonari, H., Ota, M., Ralston, A., Yabuta, N., Hirahara, S., Stephenson, R. O., Ogonuki, N. et al. (2009). The Hippo signaling pathway components Lats and Yap pattern Tead4 activity to distinguish mouse trophectoderm from inner cell mass. *Dev. Cell* **16**, 398-410.
Ota, M. and Sasaki, H. (2008). Mammalian Tead proteins regulate cell proliferation and contact inhibition as a transcriptional mediator of Hippo signaling. *Development* **135**, 4059-4069.
Pan, D. (2007). Hippo signaling in organ size control. *Genes Dev.* **21**, 886-897.
Reddy, B. V. and Irvine, K. D. (2008). The Fat and Warts signaling pathways: new insights into their regulation, mechanism and conservation. *Development* **135**, 2827-2838.
Robinson, B. S., Huang, J., Hong, Y. and Moberg, K. H. (2010). Crumbs regulates Salvador/Warts/Hippo signaling in *Drosophila* via the FERM-domain protein Expanded. *Curr. Biol.* **20**, 582-590.
Sansores-Garcia, L., Bossuyt, W., Wada, K., Yonemura, S., Tao, C., Sasaki, H. and Halder, G. (2011). Modulating F-actin organization induces organ growth by affecting the Hippo pathway. *EMBO J.* **30**, 2325-2335.
Sasaki, H., Hui, C., Nakafuku, M. and Kondoh, H. (1997). A binding site for Gli proteins is essential for HNF-3beta floor plate enhancer activity in transgenics and can respond to Shh in vitro. *Development* **124**, 1313-1322.
Saucedo, L. J. and Edgar, B. A. (2007). Filling out the Hippo pathway. *Nat. Rev. Mol. Cell Biol.* **8**, 613-621.
Sawada, A., Kiyonari, H., Ukita, K., Nishioka, N., Imuta, Y. and Sasaki, H. (2008). Redundant roles of Tead1 and Tead2 in notochord development and the regulation of cell proliferation and survival. *Mol. Cell. Biol.* **28**, 3177-3189.
Schlegelmilch, K., Mohseni, M., Kirak, O., Pruszak, J., Rodriguez, J. R., Zhou, D., Kreger, B. T., Vasioukhin, V., Avruch, J., Brummelkamp, T. R. et al. (2011). Yap1 acts downstream of alpha-catenin to control epidermal proliferation. *Cell* **144**, 782-795.
Silva, E., Tsatskis, Y., Gardano, L., Tapon, N. and McNeill, H. (2006). The tumor-suppressor gene fat controls tissue growth upstream of expanded in the hippo signaling pathway. *Curr. Biol.* **16**, 2081-2089.
Silvis, M. R., Kreger, B. T., Lien, W. H., Klezovitch, O., Rudakova, G. M., Camargo, F. D., Lantz, D. M., Seykora, J. T. and Vasioukhin, V. (2011). {alpha}-catenin is a tumor suppressor that controls cell accumulation by regulating the localization and activity of the transcriptional coactivator Yap1. *Sci. Signal.* **4**, ra33.
Striedinger, K., VandenBerg, S. R., Baia, G. S., McDermott, M. W., Gutmann, D. H. and Lal, A. (2008). The neurofibromatosis 2 tumor suppressor gene product, merlin, regulates human meningioma cell growth by signaling through YAP. *Neoplasia* **10**, 1204-1212.
Tyler, D. M. and Baker, N. E. (2007). Expanded and fat regulate growth and differentiation in the *Drosophila* eye through multiple signaling pathways. *Dev. Biol.* **305**, 187-201.
Varelas, X., Samavarchi-Tehrani, P., Narimatsu, M., Weiss, A., Cockburn, K., Larsen, B. G., Rossant, J. and Wrana, J. L. (2010). The Crumbs complex couples cell density sensing to Hippo-dependent control of the TGF-beta-SMAD pathway. *Dev. Cell* **19**, 831-844.
Wang, W., Huang, J. and Chen, J. (2010). Angiomotin-like proteins associate with and negatively regulate YAP1. *J. Biol. Chem.* **286**, 4364-4370.
Willecke, M., Hamaratoglu, F., Kango-Singh, M., Udan, R., Chen, C. L., Tao, C., Zhang, X. and Halder, G. (2006). The fat cadherin acts through the hippo tumor-suppressor pathway to regulate tissue size. *Curr. Biol.* **16**, 2090-2100.
Yi, C., Troutman, S., Fera, D., Stemmer-Rachamimov, A., Avila, J. L., Christian, N., Luna Persson, N., Shimono, A., Speicher, D. W., Marmorstein, R. et al. (2011). A tight junction-associated Merlin-Angiomotin complex mediates Merlin's regulation of mitogenic signaling and tumor suppressive functions. *Cancer Cell* **19**, 527-540.
Yoshida, T. (2008). MCAT elements and the TEF-1 family of transcription factors in muscle development and disease. *Arterioscler. Thromb. Vasc. Biol.* **28**, 8-17.
Zhang, J., Smolen, G. A. and Haber, D. A. (2008). Negative regulation of YAP by LATS1 underscores evolutionary conservation of the *Drosophila* Hippo pathway. *Cancer Res.* **68**, 2789-2794.
Zhao, B., Wei, X., Li, W., Udan, R. S., Yang, Q., Kim, J., Xie, J., Ikenoue, T., Yu, J., Li, L. et al. (2007). Inactivation of YAP oncoprotein by the Hippo pathway is involved in cell contact inhibition and tissue growth control. *Genes Dev.* **21**, 2747-2761.
Zhao, B., Li, L., Lu, Q., Wang, L. H., Liu, C. Y., Lei, Q. and Guan, K. L. (2011). Angiomotin is a novel Hippo pathway component that inhibits YAP oncoprotein. *Genes Dev.* **25**, 51-63.